

Supplementary Information

for

Dynamic Ruffling Distortion of the Heme Substrate in
Non-Canonical Heme Oxygenase Enzymes

Amanda B. Graves, Erik H. Horak, and Matthew D. Liptak

Contents

Supplemental Experimental and Results		
Table S1	F23A MhuD Mutagenic Primer Sequence	S2-S3
Table S2	F23W MhuD Mutagenic Primer Sequence	S3
Table S3	F23A MhuD Gene Sequence	S4
Table S4	F23W MhuD Gene Sequence	S5
Table S5	WT Isdl Gene Sequence	S6
Table S6	UV CD Secondary Structure Analysis	S7
Figure S1	F23A MhuD SDS-PAGE gel	S7
Figure S2	F23W MhuD SDS-PAGE gel	S8
Figure S3-S4	WT Isdl SDS-PAGE gels	S8-9
Figure S5	Structure used for Calculations	S9
Figure S6	CD Spectra of WT, F23A, and F23W MhuD	S9

CD Spectroscopy.

Experimental

To determine the effect of the F23X mutations on the fold of MhuD, UV CD spectra were collected on WT MhuD–heme–CN, F23A MhuD–heme–CN, and F23W MhuD–heme–CN between 240 and 190 nm in quartz cuvettes. The cyanide-inhibited, heme bound species were prepared as described in the main text. The species were exchanged into 50 mM Kpi, pH 7.4 with no NaCl using a PD-10 column (GE Healthcare). The samples were then further diluted with Milli-Q water to contain 10 mM KPi, pH 7.4. The measurements were performed on a Jasco J-815 spectropolarimeter averaging 5 scans with a scanning speed of 20 nm/min, a bandwidth of 1 nm, a digital integration time of 8 s, and a data pitch of 0.5 nm.

Results

UV CD was utilized to monitor if the substitutions to Phe23 affected the secondary structure of the polypeptide. UV CD can be analyzed to assess the percentage of α -helices and β -sheets comprising the protein secondary (Figure S5).¹ The cyanide-inhibited versions of the species were studied to ensure the enzyme was inactive for the experiment. The UV CD spectra for WT, F23A, and F23W MhuD–heme–CN display a peak maximum of 191 nm. WT and F23W cross through the zero line at 198 nm and F23A is shifted to 197 nm. A negative band at 209 nm is observed for WT and F23A MhuD but is found at 208 nm for F23W MhuD. Because of the differences observed between WT, F23A, and F23W MhuD, the data was analyzed with SELCON3 using IBasis=4 in the CDPro software package,²⁻⁶ and the newly developed BestSel program for deconvolution of the curves to percentage α helices and β -sheets (Table S__).⁷ The WT SELCON3 data was previously compared to the X-ray crystal structure of WT MhuD–heme–CN (PDB 4NL5) and found to have no significant changes to the structure.⁸ The SELCON3 analysis reveals a constant percentage of β -sheets between the species and a slight increase in α -helices from WT to F23A to F23W MhuD. The BestSel analysis provides UV CD WT fold values closer to the X-ray crystallography attained

values. The F23A and F23W MhuD variants change only by 2% at most compared to WT MhuD when analyzed by the BestSel program. As the mutations do not significantly affect the protein secondary structure the changes to the electronic structure of the heme are due to changes to the second coordination sphere and not due to the protein unfolding.

- 1 Greenfield, N. J. *Nat. Proto.* 2006, **1**, 2876-2890.
- 2 Sreerama, N.; Woody, R. W. *Anal. Biochem.* 1993, **209**, 32-44.
- 3 Sreerama, N.; Woody, R. W. *Biochemistry* 1994, **33**, 10022-10025.
- 4 Sreerama, N.; Venyaminov, S. Y.; Woody, R. W. *Protein Sci.* 1999, **8**, 370-380.
- 5 Sreerama, N.; Woody, R. W. *Anal. Biochem.* 2000, **287**, 252-260.
- 6 Johnson, W. C. *Proteins* 1999, **35**, 307-312.
- 7 Micsonai, A.; Wien, F.; Kernya, L.; Lee, Y. H.; Goto, Y.; Refregiers, M.; Kardos, P. *Natl. Acad. Sci. USA*. 2015, **112**, 3095-3103.
- 8 Graves, A. B.; Morse, R. P.; Chao, A.; Iniguez, A.; Goulding, C. W.; Liptak, M. D. *Inorg. Chem.* 2014, **53**, 5931-5940.

Table S1. F23A MhuD mutagenic primer

Primer	Sequence
Forward	5'-GCTGGAGAAGCGGGCCGCTCACCGCGCG -3'
Reverse	5'-CGCGCGGTGAGCGGCCCGCTTCTCCAGC -3'

Table S2. F23W MhuD mutagenic primer

Primer	Sequence
Forward	5'-GCTGGAGAAGCGGGTGGGCTCACCGCGCG -3'
Reverse	5'-CGCGCGGTGAGCCCACCGCTTCTCCAGC-3'

Table S3. F23A MhuD gene sequence

M1 ATG	P2 CCA	V3 GTG	V4 GTG	K5 AAG	I6 ATC	N7 AAC	A8 GCA	I9 ATC
E10 GAG	V11 GTG	P12 CCC	A13 GCC	G14 GGC	A15 GCT	G16 GGC	P17 CCC	E18 GAG
L19 CTG	E20 GAG	K21 AAG	R22 CGG	A23 GCC	A24 GCT	H25 CAC	R26 CGC	A27 GCG
H28 CAC	A29 GCG	V30 GTC	E31 GAG	N32 AAC	S33 TCC	P34 CCG	G35 GGT	F36 TTC
L37 CTC	G38 GGC	F39 TTT	Q40 CAG	L41 CTG	L42 TTA	R43 CGT	P44 CCG	V45 GTC
K46 AAG	G47 GGT	E48 GAA	E49 GAA	R50 CGC	Y51 TAC	F52 TTC	V53 GTG	V54 GTG
T55 ACA	H56 CAC	W57 TGG	E58 GAG	S59 TCC	D60 GAT	E61 GAA	A62 GCA	F63 TTC
Q64 CAG	A65 GCG	W66 TGG	A67 GCA	N68 AAC	G69 GGG	P70 CCC	A71 GCC	I72 ATC
A73 GCA	A74 GCC	H75 CAT	A76 GCC	G77 GGA	H78 CAC	R79 CGG	A80 GCC	N81 AAC
P82 CCC	V83 GTG	A84 GCG	T85 ACC	G86 GGT	A87 GCT	S88 TCG	L89 CTG	L90 CTG
E91 GAA	F92 TTC	E93 GAG	V94 GTC	V95 GTG	L96 CTT	D97 GAC	V98 GTC	G99 GGT
G100 GGG	T101 ACC	G102 GGC	K103 AAG	T104 ACT	A105 GCA	G106 GGA	G107 GGT	V108 GTA
P109 CCA	R110 CGA	G111 GGT	K112 AAG	L113 CTT	A114 GCG	A115 GCC	A116 GCA	L117 CTC
E118 GAG	H119 CAC	H120 CAC	H121 CAC	H122 CAC	H123 CAC	H124 CAC		

Table S4. F23W MhuD gene sequence

M1 ATG	P2 CCA	V3 GTG	V4 GTG	K5 AAG	I6 ATC	N7 AAC	A8 GCA	I9 ATC
E10 GAG	V11 GTG	P12 CCC	A13 GCC	G14 GGC	A15 GCT	G16 GGC	P17 CCC	E18 GAG
L19 CTG	E20 GAG	K21 AAG	R22 CGG	W23 TGG	A24 GCT	H25 CAC	R26 CGC	A27 GCG
H28 CAC	A29 GCG	V30 GTC	E31 GAG	N32 AAC	S33 TCC	P34 CCG	G35 GGT	F36 TTC
L37 CTC	G38 GGC	F39 TTT	Q40 CAG	L41 CTG	L42 TTA	R43 CGT	P44 CCG	V45 GTC
K46 AAG	G47 GGT	E48 GAA	E49 GAA	R50 CGC	Y51 TAC	F52 TTC	V53 GTG	V54 GTG
T55 ACA	H56 CAC	W57 TGG	E58 GAG	S59 TCC	D60 GAT	E61 GAA	A62 GCA	F63 TTC
Q64 CAG	A65 GCG	W66 TGG	A67 GCA	N68 AAC	G69 GGG	P70 CCC	A71 GCC	I72 ATC
A73 GCA	A74 GCC	H75 CAT	A76 GCC	G77 GGA	H78 CAC	R79 CGG	A80 GCC	N81 AAC
P82 CCC	V83 GTG	A84 GCG	T85 ACC	G86 GGT	A87 GCT	S88 TCG	L89 CTG	L90 CTG
E91 GAA	F92 TTC	E93 GAG	V94 GTC	V95 GTG	L96 CTT	D97 GAC	V98 GTC	G99 GGT
G100 GGG	T101 ACC	G102 GGC	K103 AAG	T104 ACT	A105 GCA	G106 GGA	G107 GGT	V108 GTA
P109 CCA	R110 CGA	G111 GGT	K112 AAG	L113 CTT	A114 GCG	A115 GCC	A116 GCA	L117 CTC
E118 GAG	H119 CAC	H120 CAC	H121 CAC	H122 CAC	H123 CAC	H124 CAC		

Table S5. WT lsdl gene sequence.

M1 ATG	F2 TTT	M3 ATG	A4 GCA	E5 GAA	N6 AAT	R7 AGA	L8 TTA	Q9 CAA
L10 TTA	Q11 CAA	K12 AAA	G13 GGC	S14 AGT	A15 GCG	E16 GAA	E17 GAA	T18 ACG
I19 ATT	E20 GAA	R21 CGT	F22 TTT	Y23 TAC	N24 AAT	R25 AGA	Q26 CAA	G27 GGT
I28 ATT	E29 GAA	T30 ACT	I31 ATT	E32 GAA	G33 GGC	F34 TTC	Q35 CAA	Q36 CAA
M37 ATG	F38 TTT	V39 GTC	T40 ACT	K41 AAA	T42 ACA	L43 TTA	N44 AAT	T45 ACC
E46 GAG	D47 GAT	T48 ACA	D49 GAC	E50 GAA	V51 GTT	K52 AAA	I53 ATC	L54 TTA
T55 ACT	I56 ATT	W57 TGG	E58 GAA	S59 TCT	E60 GAA	D61 GAT	S62 AGC	F63 TTT
N64 AAT	N65 AAT	W66 TGG	L67 TTG	N68 AAT	S69 TCC	D70 GAT	V71 GTA	F72 TTT
K73 AAA	E74 GAA	A75 GCT	H76 CAT	K77 AAA	N78 AAT	V79 GTA	R80 CGT	L81 TTA
K82 AAA	S83 AGT	D84 GAT	D85 GAC	D86 GAT	G87 GGA	Q88 CAG	Q89 CAA	S90 AGT
P91 CCA	I92 ATA	L93 TTA	S94 TCA	N95 AAT	K96 AAA	V97 GTA	F98 TTC	K99 AAA
Y100 TAT	D101 GAT	I102 ATT	G103 GGC	Y104 TAC	H105 CAC	Y106 TAT	Q107 CAA	K108 AAA

Table S6. Secondary structure analysis by UV CD for MhuD–heme–CN variants

Species	Percent α helical	Percent β sheet
WT ^a	14.0	21.0
F23A ^a	23.0	22.0
F23W ^a	27.0	21.0
WT ^b	21.0	31.0
F23A ^b	22.0	29.5
F23W ^b	20.9	33.4
WT ^c	19.0	31.0

^a Analyzed with Selcon3²⁻⁶ ^b Analyzed with BestSel⁷ ^c From X-ray crystal structure (PDB 4NL5)⁸

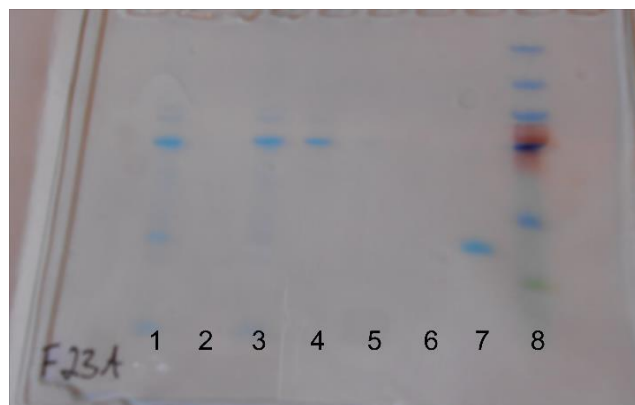


Figure S1. SDS-PAGE gel of F23A MhuD. 50 mM Tris, pH 7.4, 50 mM NaCl, 25 mM imidazole wash (1), 50 mM Tris, pH 7.4, 50 mM NaCl, 50 mM imidazole wash (2), 50 mM Tris, pH 7.4, 50 mM NaCl, 75 mM imidazole wash (3), 50 mM Tris, pH 7.4, 50 mM NaCl, 100 mM imidazole wash (4), 1/100 dilution of F23A MhuD (5), 1/10 dilution of F23A MhuD (6), Pure F23A MhuD (7), and molecular weight ladder (8).

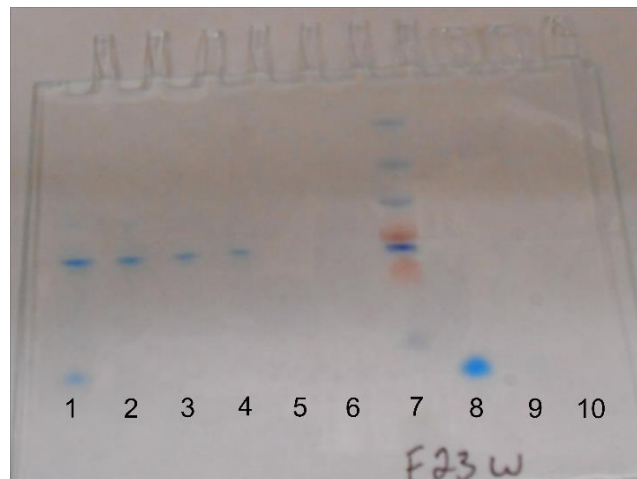


Figure S2. SDS-PAGE gel of F23W MhuD. Lysate (1), column flow through (2), 50 mM Tris, pH 7.4, 50 mM NaCl, 25 mM imidazole wash (3), 50 mM Tris, pH 7.4, 50 mM NaCl, 50 mM imidazole wash (4), 50 mM Tris, pH 7.4, 50 mM NaCl, 75 mM imidazole wash (5), 50 mM Tris, pH 7.4, 50 mM NaCl, 100 mM imidazole wash (6), and molecular weight ladder (7), pure F23W MhuD (8), 1/10 dilution of F23W MhuD (9), 1/100 dilution of F23W MhuD (10).

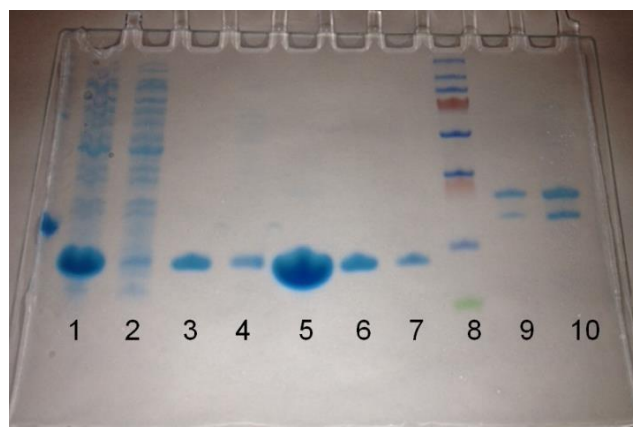


Figure S3. SDS-PAGE gel of Uncleaved WT lsdl. Lysate (1), column flow through (2), 50 mM Tris, pH 7.4, 10 mM imidazole wash (3), 50 mM Tris, pH 7.4, 150 mM NaCl, 50 mM imidazole wash (4), pure His-tagged WT lsdl (5), 1/20 dilution of pure His-tagged WT lsdl (6), 1/100 dilution of pure His-tagged WT lsdl (7), molecular weight ladder (8), TEV post-dialysis (9), TEV pre-dialysis (10).

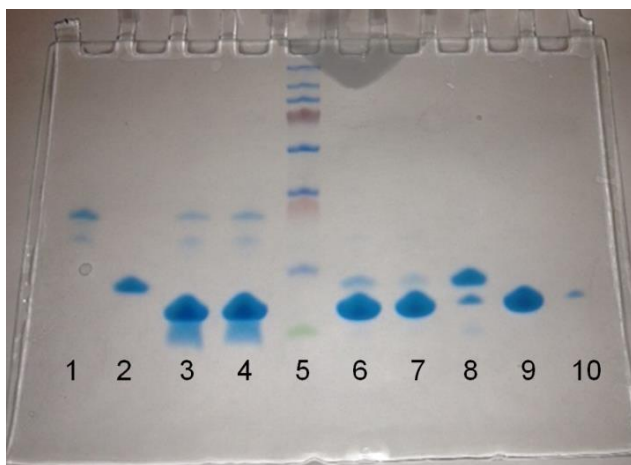


Figure S4. SDS-PAGE gel of WT lsdl cleavage with TEV. TEV post-dialysis (1), 1/20 dilution of pure His-tagged WT lsdl (2), lsdl/TEV reaction pre-dialysis (3), lsdl/TEV post-dialysis (4), molecular weight ladder (5), eluted WT lsdl in 50 mM Tris, pH 7.4 (6), 1st reloaded eluted WT lsdl (7), 50 mM Tris, pH 7.4, 10 mM imidazole wash (8), pure untagged WT lsdl (9), 1/20 dilution of pure untagged WT lsdl (10).

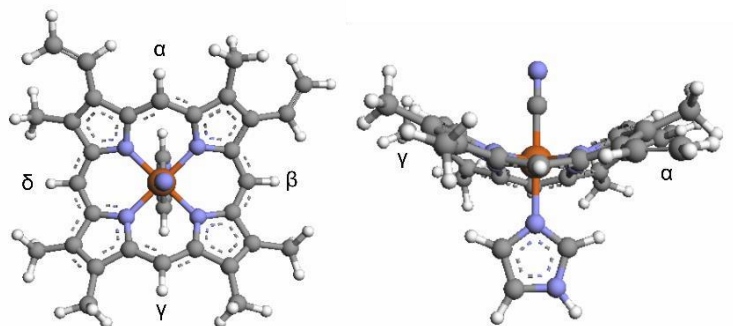


Figure S5. Computational model used for all calculations, shown with the heme ruffled to 2.2 Å. The α -meso–Fe– γ -meso angle was constrained to vary the degree of ruffling.

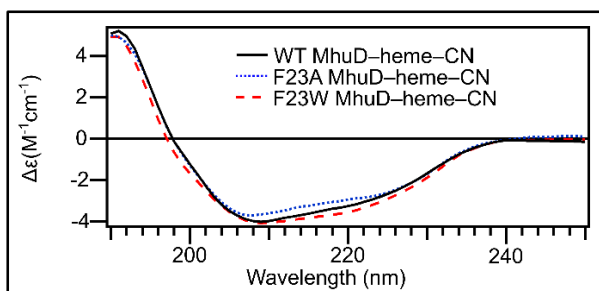


Figure S6. UV CD of WT (black, solid line), F23A (blue, dotted line), and F23W MhuD–heme–CN (red, dashed line) for secondary structural analysis. All collected in 10 mM KPi, pH 7.4